ChemPubSoc Europe

DOI: 10.1002/cmdc.201600213

CHEMMEDCHEM Full Papers

Synthesis and Biological Evaluation of Iodoglucoazomycin (I-GAZ), an Azomycin–Glucose Adduct with Putative Applications in Diagnostic Imaging and Radiotherapy of Hypoxic Tumors

Piyush Kumar,*[a] Hassan R. H. Elsaidi,[a, b] Bohdarianna Zorniak,[a] Evelyn Laurens,[c] Jennifer Yang,[a] Veena Bacchu,[a] Monica Wang,[a] and Leonard I. Wiebe[a]

Iodoglucoazomycin (I-GAZ; *N*-(2-iodo-3-(6-*O*-glucosyl)propyl)-2-nitroimidazole), a non-glycosidic nitroimidazole–6-*O*-glucose adduct, was synthesized, radioiodinated, and evaluated as a substrate of glucose transporter 1 (GLUT1) for radiotheranostic (therapy + diagnostic) management of hypoxic tumors. Nucleophilic iodination of the nosylate synthon of I-GAZ followed by deprotection afforded I-GAZ in 74% overall yield. I-GAZ was radioiodinated via 'exchange' labeling using [$^{123/131}$I]iodide (50–70% RCY) and then purified by Sep-Pak™ (>96% RCP). [^{131}I]I-GAZ was stable in 2% ethanolic solution in sterile water for 14 days when stored at 5 °C. In cell culture, I-GAZ was found to be nontoxic to EMT-6 cells at concentrations <0.5 mM, and weakly radiosensitizing (SER 1.1 at 10% survival of EMT-6 cells; 1.2 at 0.1% survival in MCF-7 cells). The hypoxic/normoxic uptake ratio of [^{123}I]I-GAZ in EMT-6 cells was 1.46 at 2 h, and under normoxic conditions the uptake of [^{123}I]I-GAZ by EMT-6 cells was unaltered in the presence of 5 mM glucose. The biodistribution of [^{131}I]I-GAZ in EMT-6 tumor-bearing Balb/c mice demonstrated rapid clearance from blood and extensive renal and hepatic excretion. Tumor/blood and tumor/muscle ratios reached ~3 and 8, respectively, at 4 h post-injection. Regression analysis of the first order polynomial plots of the blood and tumor radioactivity concentrations supported a perfusion–excretion model with low hypoxia-dependent binding. [^{131}I]I-GAZ was found to be stable in vivo, and did not deiodinate.

Introduction

Cellular molecular responses to focal tissue hypoxia are critical to the development and prognosis of several clinical pathologies, including cancer,[1] liver disease,[2] myocardial and peripheral vascular diseases,[3] diabetes[4] and arthritis.[5] In cancer, electron-affinic, bioreductively activated oxygen-mimetics, particularly the 2-nitroimidazoles (2-NI; azomycin) have been investigated as radiosensitizer adjuncts for X-ray radiotherapy of radioresistant hypoxic cells[6–8] and as imaging diagnostics of hypoxic tumor.[9–14] In general, these radiosensitizers have failed to perform effectively as neo-adjuvants to radiation therapy. In the case of nitroimidazoles, the narrow therapeutic window and related dose-limiting toxicities have contributed to their clinical ineffectiveness.[15] For imaging focal hypoxia, however, the nitroimidazole-based radiotracers have been effective. Several PET tracers, including fluorine-18-fluoromisonidazole ([^{18}F]FMISO)[16] and fluorine-18-fluoroazomycin arabino-

[a] Prof. Dr. P. Kumar, Dr. H. R. H. Elsaidi, B. Zorniak, J. Yang, Dr. V. Bacchu, M. Wang, Prof. Dr. L. I. Wiebe
Department of Oncology, Cross Cancer Institute,
University of Alberta, University Ave., Edmonton, AB, T6G 1Z2 (Canada)
E-mail: pkumar@ualberta.ca

[b] Dr. H. R. H. Elsaidi
Department of Pharmaceutical Chemistry,
Faculty of Pharmacy, University of Alexandria,
El Sultan Hussein St. Azarita, Alexandria (Egypt)

[c] Dr. E. Laurens
Clinical Imaging Research Centre,
14 Medical Drive, #B1-01, Singapore 117599 (Singapore)

Supporting information and the ORCID identification number(s) for the author(s) of this article can be found under http://dx.doi.org/10.1002/cmdc.201600213.

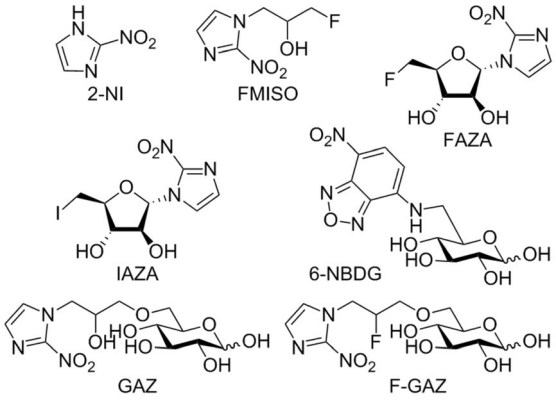

Figure 1. Structures of 2-NI (azomycin), FMISO, FAZA, IAZA, 6-NDBG, GAZ, and F-GAZ.

side ([^{18}F]FAZA),[17,18] and the SPECT agent iodine-123-iodoazomycin arabinoside ([^{123}I]IAZA)[19] have found extensive clinical use in hypoxia detection in cancer imaging (Figure 1). Although these agents have performed well enough to justify their continued use in patient studies, all, without exception, achieve relatively low target-background concentration ratios and hence lead to low-contrast images.[12] Their performance as imaging agents reflects their diffusion-based local delivery to hypoxic cells (i.e., pharmacokinetics) and to a lesser extent, their oxygen-dependent binding rates (i.e., electron affinity).[7,20–24] Their poor performance as in vivo radiosensitizers when used in conjunction with X-ray treatment has been attributed to their inability to achieve radiosensitizing concentrations at dose-limiting neurotoxicities.[25] The consensus remains that there is still a clinical need for more effective radiosensitizers.[26]

Approaches to obtaining more rapid, hypoxia-sensitive uptake of electron-affinic nitroimidazole derivatives by hypoxic cells have focused on exploitation of equilibrative and concentrative transmembrane transport proteins, including nucleoside transporters,[23] amino-acid transporters[27] and glucose transporters (GLUTs).[28–30] For example, the design of selected glucose-C6-*O*-azomycin adducts[29,30] was rationalized from the reported GLUT1 transport of the corresponding C6-*O*-glucose–NBD adduct, 6-NBDG.[31]

GLUTs are particularly attractive transport elements to support imaging and/or molecular radiotherapy (MRT) of hypoxia because several GLUT subtypes, including GLUT1, are upregulated in hypoxic cells.[32] The parent compound of the glucose-C6-*O*-azomycin adduct series, *N*-(2-hydroxy-3-(6-*O*-glucosyl)-propyl)-2-nitroimidazole (GAZ), was found to be nontoxic but only weakly radiosensitizing to hypoxic cells in cell culture.[29] The fluoro analogue, F-GAZ (*N*-(2-fluoro-3-(6-*O*-glucosyl)propyl)-2-nitroimidazole; fluoroglucoazomycin), was weakly competitive against [^{18}F]FDG uptake in cell culture, and therefore considered to accumulate independently of transport via GLUT1. However in PET imaging studies, [^{18}F]F-GAZ did delineate hypoxic tumor in a murine model.[30] EMT-6 tumors, despite rapid renal clearance kinetics of [^{18}F]F-GAZ, exhibited prolonged retention of low levels radioactivity (~1% ID/g at 60 min) after injection of carrier-added (100 mg kg^{-1}) doses. This indicates that these compounds have potential for use as adjunct therapeutics (i.e., as radiosensitizers) for external beam radiotherapy (XRT), or as molecular radiotherapeutics (MRT) to supplement XRT if radiotherapeutic radionuclides were used in place of fluorine-18.[30] The current work describes the synthesis, radiolabeling chemistry, in vitro biology and in vivo biodistribution of I-GAZ (*N*-(2-iodo-3-(6-*O*-glucosyl)propyl)-2-nitroimidazole; iodoglucoazomycin). I-GAZ is more lipophilic than GAZ and F-GAZ and was therefore expected to display altered pharmacokinetics that could lead to improved uptake in target tissues.

Results and Discussion

Chemistry and radiolabeling

As depicted in Scheme 1, synthesis of the target compound, I-GAZ, was achieved starting from the advanced intermediate, **1**, which was previously synthesized in our laboratory.[29] Treatment of nosylate **1** with sodium iodide in DMF followed by in situ acetolysis of the resulting product using 0.1 M methanolic sodium methoxide afforded I-GAZ in 74% yield over two steps. The structure of the target compound was confirmed using ^{1}H NMR, ^{13}C NMR spectroscopies and high-resolution mass spectrometry (HRMS).

Radioiodine exchange radiolabeling of cold I-GAZ was selected as the preferred labeling method. A number of preliminary reactions with various solvents [acetonitrile, 1,2-dimethoxyethane (DME), dimethyl sulfoxide (DMSO), *N*,*N*-dimethylformamide (DMF), methyl ethyl ketone (MEK)], with and without pivalic acid (data not shown) led to the selection of exchange radioiodination using pivalic acid melt conditions,[33] followed by recovery and purification by Sep-Pak™ filtration, to afford the labeled radiopharmaceutical in radiochemical yields (RCY) of 50–70% and radiochemical purities of 96–99%. The purification of [$^{123/131}$I]I-GAZ by Sep-Pak™ filtration was a priority given the simplicity of the method in comparison with HPLC, particularly in light of contamination/decontamination of HPLC columns and equipment encountered when using the longer-lived radioiodine isotopes (i.e., iodine-131 $t_{1/2}$~8.02 d) which make the 'single use' Sep-Pak™ technology ideal for this work. However, for stability studies, both Sep-Pak™ [^{131}I]I-GAZ and HPLC-purified [^{131}I]I-GAZ were used. They were individually dissolved in 2% EtOH in sterile water and stored in the dark at 22 °C for 7 days. Periodic (24 h, 72 h, and 7 d) radio-TLC analyses revealed that the radiochemical purity (RCP) of [^{131}I]I-GAZ samples purified by either procedure remained unchanged (Figure 2).

In vitro evaluations of I-GAZ

Previous investigations of this class of halo-glucose–nitroimidazole adducts showed that these compounds were weakly cyto-

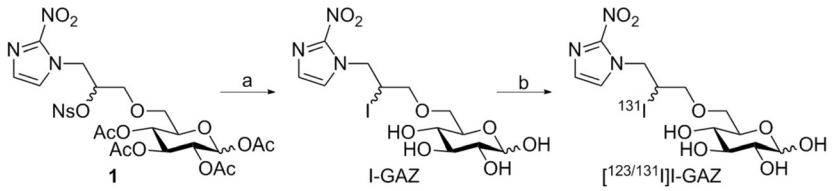

Scheme 1. Synthesis of I-GAZ and [$^{123/131}$I]I-GAZ: a) 1. NaI, DMF, 60 °C, 3 h; 2. 0.1 M $NaOCH_3$, CH_3OH/CH_2Cl_2, 74% (two steps); b) pivalic acid melt, Na[$^{123/131}$I] exchange.

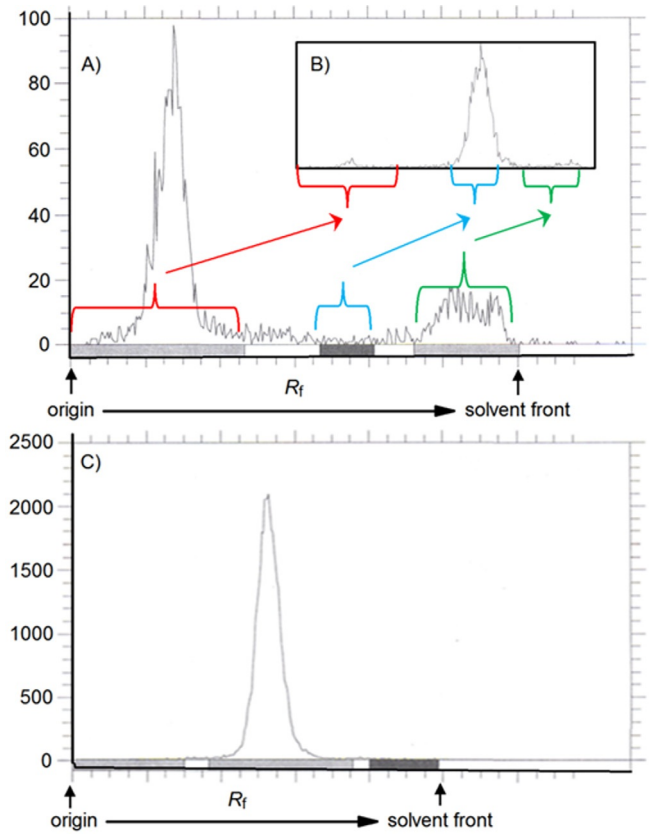

Figure 2. A) A TLC radiochromatogram depicts the first elution of a Sep-Pak™ cartridge loaded with the radioiodination reaction mixture following deprotection of crude [^{131}I]I-GAZ, and B) the inset depicts a TLC radiochromatogram of the second elution of the same Sep-Pak™ cartridge. C) TLC radiochromatogram for a sample of purified [^{131}I]I-GAZ after 14 days storage in 2% ethanolic sterile water for injection at 22 °C.

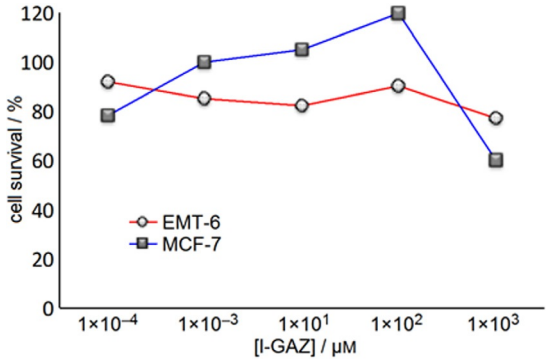

Figure 3. Cytotoxicity of I-GAZ against EMT-6 and MCF-7 cells incubated in air (with 5% CO_2). Plotted survival data are normalized to cell numbers in wells containing no I-GAZ, i.e., 100% cell survival.

toxic, with inhibitory concentrations (IC_{50}) in the 0.5 mM range and with low uptake under cell culture conditions.[29,30] I-GAZ toxicity was similarly apparent at concentrations of 0.5 mM and greater, as shown (Figure 3). This was in line with the long-standing concept that nitroimidazoles have a preferential toxicity toward hypoxic rather than normoxic cells, and that this toxicity arises through the formation of several bioreduced intermediates of the nitro moiety.[34–38]

In vitro radiosensitization

In vitro radiosensitizer potency may be expressed as the sensitizer enhancement ratio (SER). In vitro SERs are often determined at relatively high concentrations (i.e., 1 mM),[39] but the toxicity of the putative radiosensitizer must be considered when conducting these experiments. For I-GAZ, it was determined that a concentration of 0.5 mM could be used with minimal cytotoxicity. The radiosensitization (SER ~ 1.1) induced by I-GAZ at this concentration would appear to preclude effective in vivo radiosensitization. In the current work, normoxic/hypoxic SER data for EMT-6 cells could only be measured at the 10% cell survival levels, which would be too high for meaningful interpretation or application using in vivo models. Lower surviving fractions, say < 1%, would have required high radiation doses that the radiation source available for this work could not deliver within a reasonable time frame. Nonetheless, the oxygen enhancement ratio (OER) measured at the 10% survival dose was ~3, thereby validating the experiment procedure (Figure 4).

Data for MCF-7 cells indicated an OER of ~2.3, and a SER of ~1.2 at an I-GAZ concentration of 0.5 mM (Table 1). Target SERs of 1.5–1.8 have been reported for several 2-nitroimidazoles in cell culture, for radiosensitizer concentrations of 1.6 mM.[7]

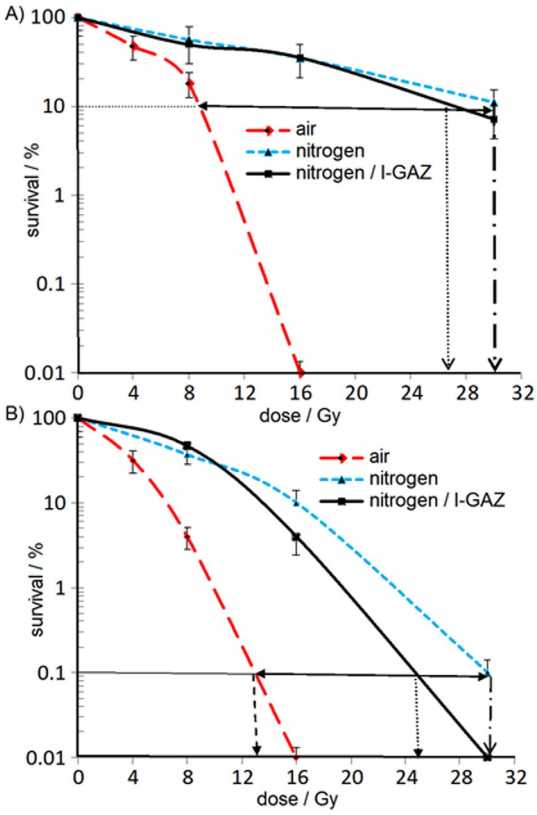

Figure 4. Radiosensitization of A) EMT-6 and B) MCF-7 cells in vitro by I-GAZ (0.5 mM). Data are plotted as percentages of the normalized surviving fraction; error bars depict 1 standard deviation ($n = 4$ for controls, i.e., no radiation; $n = 3$ for irradiated cultures). Vertical drop-lines point to radiation doses (Gy) for the respective survival level (10 and 1% for EMT-6 and MCF-7, respectively) for each treatment (air, nitrogen, nitrogen with I-GAZ) were used to calculate OER and SER for each cell line.

Table 1. Summary of I-GAZ toxicity, radiosensitization, and cell uptake in cell culture.

Cell line	IC_{50} [mM]	OER (survival [%])[a]	SER (survival [%])[b]	N_2/air I-GAZ uptake ratio[c]	Glucose inhibition of I-GAZ uptake [%][d]
EMT-6	>1	~3 (10)	1.1 (10)	1.46	6
MCF-7	>1	2.3 (0.1)	1.2 (0.1)	ND	ND

[a] Determined at 0.5 mM I-GAZ. [b] pmol [^{123}I]I-GAZ per 10^6 cells in 2 h incubations under nitrogen or air; the corresponding value for [^{123}I]IAZA was 5.35. [c] [^{123}I]I-GAZ uptake in the presence of 5 mM (glucose / no glucose) × 100, determined after 60 min incubation; data are standardized per mg protein. The corresponding value for [^{18}F]FDG under these conditions was 38% inhibition. [d] ND: not determined.

Clearly, determination of the radiosensitization properties and sensitization efficiency of I-GAZ in vitro and in vivo, including measurement of its in vivo intratumor concentrations would be required.

In vitro I-GAZ–GLUT interaction

The glucose–nitroimidazole adduct family of radiosensitizers was initially designed to be transported into cells by GLUT proteins.[28] Studies of F-GAZ competition with [^{18}F]FDG indicated that F-GAZ is a weak competitor for transport, especially in the presence of physiological concentrations of glucose in cell culture.[29]

In the current work, [^{123}I]I-GAZ and [^{18}F]FDG were incubated in vitro in EMT-6 cell culture to provide further clarification of the I-GAZ-GLUT interaction, this time using glucose at either physiological or decreased (nominally zero, as no glucose was included in the culture medium during the experiments) concentrations as the competitive substrate (Figure 5).

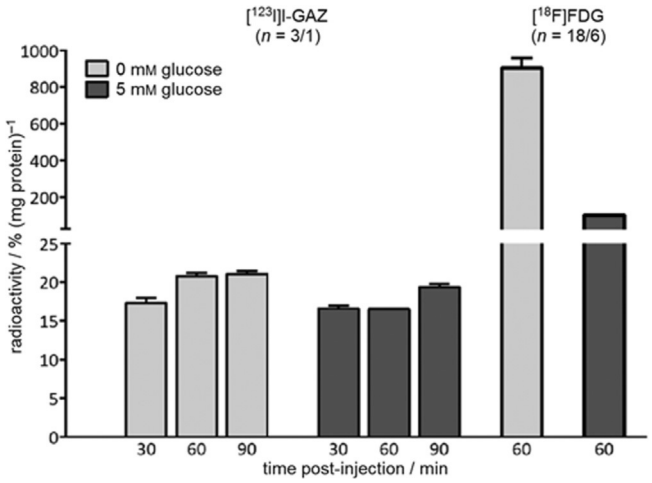

Figure 5. Uptake of [^{123}I]I-GAZ by EMT-6 cells in cell culture in the presence (5 mM) or absence of glucose. Uptake of [^{18}F]FDG is shown for comparison. Data are the mean ± SD, $n = 3$; error bars depict one SD.

Biodistribution of radioactivity (BR)

BR in tissues of Balb/c mice bearing implanted EMT-6 tumors was determined periodically over 24 h following a bolus intravenous (i.v.) injection of [^{131}I]I-GAZ. In general, the data depict low penetration into soft tissues (muscle, adipose tissue, pancreas and spleen), and rapid entry into the hepatobiliary (liver, gall bladder and intestines) and renal (kidney) excretory organs. Radioactivity levels in stomach and thyroid remained low throughout the study period. Tumor radioactivity was intermediate between non-excretory and excretory tissues. In terms of total uptake and clearance over time, these data support a model of low extravascular distribution, rapid renal clearance attributable to the high hydrophilicity of I-GAZ, and extensive hepatobiliary clearance commensurate with its high molecular weight. Fluctuations in gall bladder radioactivity and persistent small intestine radioactivity may be an indication of enterohepatic recycling of [^{131}I]I-GAZ and/or metabolites (see the Supporting Information for detailed data).

Comparisons of concentrations in tumor/blood and tumor/muscle are indicative of hypoxia-specific uptake and retention of radioactivity in hypoxic tumor, and in turn, the possibility of using [$^{123/131}$I]I-GAZ as a tumor hypoxia imaging and in situ MRT agent (Figure 6).

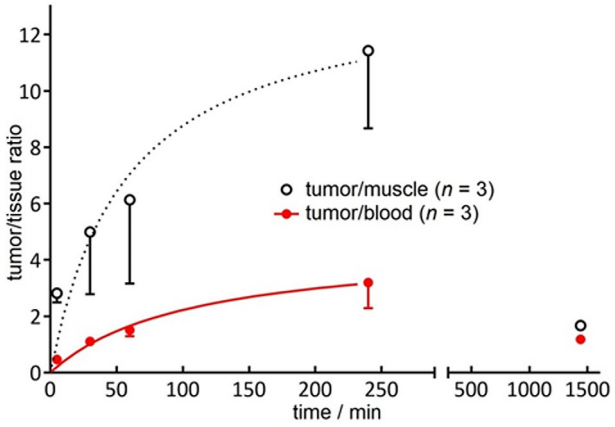

Figure 6. Relative concentration ratios of radioactivity in tumor, blood and muscle in Balb/c mice bearing implanted EMT-6 tumors, following bolus i.v. injection of [^{131}I]I-GAZ. Data are the mean ± SD, $n = 3$; error bars depict one SD.

Tumor, blood and muscle uptake of [^{131}I]I-GAZ in EMT-6 tumor-bearing Balb/c mice are compared with published data for [^{125}I]IAZA,[^{18}F]FAZA[40] and [^{18}F]F-GAZ in the same tumor model in Table 2 and Figure 7 ([^{125}I]IAZA only). All parameters measured (%ID/g, T/B and T/M) were less favorable for the GAZ derivatives than for their respective radiofluorinated/radioiodinated azomycin nucleoside analogues. These comparisons would appear to mitigate against the use of labeled I-GAZ in hypoxia imaging, even though the tumor/muscle ratios (i.e., tissue background) appear to be favorable.

Clinical data from patient tumors imaged with [^{18}F]FMISO have shown that a positive or flat slope in the immediate post-distribution phase of the tumor radioactivity/time curve was a better prognosticator of tumor intractability (i.e., the pres-

Table 2. Comparison of tumor uptake (%ID/g), tumor/muscle (T/M) and tumor/blood (T/B) ratios from biodistribution studies in a murine tumor (EMT-6) model.

Hypoxia radiotracer	[Ref.]	*t* [h] post-injection	# Animals	Uptake [%ID/g]	T/M	T/B
[^{18}F]FAZA	[40]	3	8	1.38 ± 0.62[a]	7.1 ± 2.9	9.8 ± 0.1
[^{125}I]IAZA	[33]	4	6	2.08 ± 1.24[a]	8.7	4.6 ± 0.5
[^{125}I]IAZA	[33]	24	6	0.21 ± 0.05[a]	10.3	5.6 ± 1.1
[^{18}F]F-GAZ	[30]	1	4	1.11 ± 0.16	2.2 ± 0.3	1.2 ± 0.1
[^{131}I]I-GAZ	[this work]	1	3	1.14 ± 0.19	6.1 ± 3.0	1.5 ± 0.2
[^{131}I]I-GAZ	[this work]	4	3	0.24 ± 0.06	11.4 ± 2.7	3.2 ± 0.9
[^{131}I]I-GAZ	[this work]	24	3	0.03 ± 0.00	1.7 ± 0.8	1.2 ± 0.4

[a] Mean ± SD; other values are ± SEM.

(Figure 8), i.e., a perfusion–excretion model with minimal hypoxia-dependent binding. With only a negative slope for the tumor radioactivity profile throughout the study, the Eschmann analysis, if applicable to this animal model, would indicate that in this animal model, IGAZ is not a strong diagnostic of tumor hypoxia.

Conclusions

The synthesis of unlabeled and radioiodinated I-GAZ, which were readily obtained through iodination and then deprotection of the versatile synthon

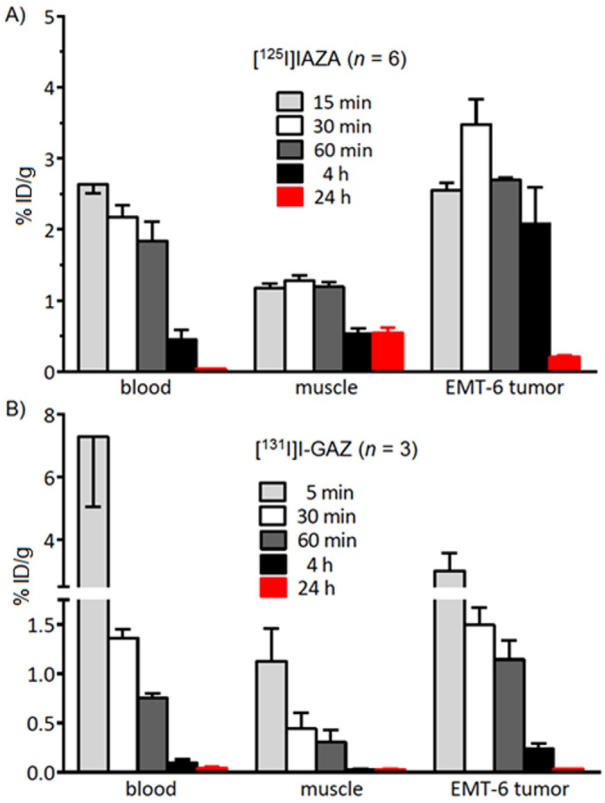

Figure 7. Biodistribution in EMT-6 tumor-bearing Balb/c mice. Radioactivity uptake and clearance over time for A) [^{125}I]IAZA ($n = 6$ for each time interval) and B) [^{131}I]I-GAZ ($n = 3$ for each time interval) following bolus i.v. injection into Balb/c mice bearing implanted EMT-6 tumors. Error bars represent one standard deviation. [^{125}I]IAZA data are adapted from Mannan et al.[33]

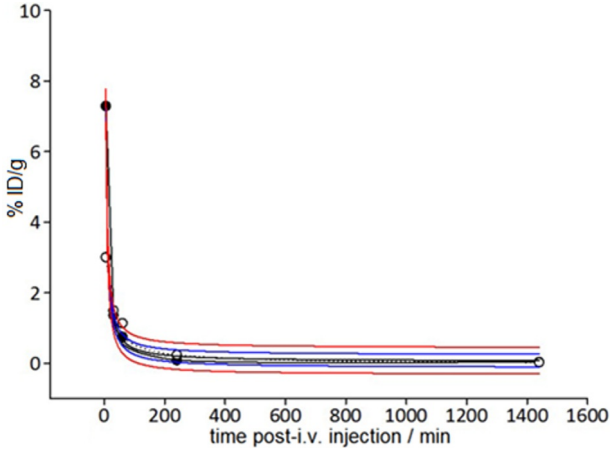

Figure 8. Analysis of clearance of radioactivity from blood (●) and tumor (○) over a 24 h period following i.v. injection of [^{131}I]I-GAZ in EMT-6 tumor-bearing Balb/c mice. The superimposed black lines essentially represent the first-order polynomial regression ($r^2 > 0.99$) for blood (solid line) and tumor (dashed). Red and blue lines represent the predicted and 95% confidence limits. Analysis was done using SigmaPlot 12; "confidence band" refers to the region of uncertainties in the predicted values over a range of values for the independent variable; prediction band refers to the region of uncertainties in predicting the response for a single additional observation at each point within a range of independent variable values. The independent variable values used to compute the confidence bands are the same values used to create the fit curve (Systat Software, Inc.).

ence of hypoxic cells) than the standardized absolute uptake of the tracer (e.g., standard uptake value, SUV_{max}).[39] In the case of [^{131}I]I-GAZ evaluation in mice, concentrations of radiotracer in EMT-6 tumor were 2–3 times higher than blood radioactivity in the 1–4 h window after injection, representing about one percent of the injected dose. However, regression analysis of the first-order polynomial plots of the blood and tumor radioactivity concentrations indicated that the clearance of [^{131}I]I-GAZ from both tissues followed a similar time course

1-α/β-D-(1,2,3,4-tetra-*O*-acetyl)-6-*O*-(9-[2-nitro-1*H*-imidazolyl]-8*R*/*S*-*O*-(4-nitrobenzenesulfonyloxy)propyl)glucopyranose (acetylglucoazomycin nosylate; Ac-GAZ-Ns) are reported. The radiolabeled product,[^{131}I]I-GAZ, was stable for at least 14 days when kept in 2% ethanol in sterile water at 22 °C.

In vitro studies showed that I-GAZ is a relatively weak radiosensitizer when tested at its in vitro IC_{50} concentration (0.5 mM), especially against EMT-6 cells (SER 1.1 at 10% survival). The SER for MCF-7 cells was ~1.2 at 1% survival. In cell culture (EMT-6 cells),[^{131}I]I-GAZ uptake was almost 50% higher under hypoxia than under air, demonstrating hypoxia-dependent binding, but cellular uptake of [^{131}I]I-GAZ was virtually independent of the presence or absence of glucose, indicating that transport by GLUT was not an important factor in its uptake. In summary, the in vitro data provide evidence of I-

GAZ bioreduction leading to higher toxicity and increased retention in hypoxic cells, as would be expected for 2-nitroimidazoles. However, I-GAZ was only a weak radiosensitizer of EMT-6 and MCF-7 cells under the prescribed experimental conditions. The independence of cell uptake on the presence or absence of glucose in the culture medium was taken as evidence that I-GAZ uptake is not GLUT-mediated.

In vivo biodistribution studies of [^{131}I]I-GAZ in Balb/c mice with implanted EMT-6 tumors provided evidence for rapid clearance from blood, extensive renal but predominantly hepatic excretion, and stability against deiodination. Tumor/blood ratios exceeded unity within 30 min, and rose to ~3 at 4 h, whereas tumor/muscle ratios rose from ~3 over the first h, to ~8 at 4 h post-injection. Analysis of temporal blood and tumor radioactivity after injection revealed quantitative similarities between the two sets of data (Figure 8).

Experimental Section

General synthesis methods: Solvents used in reactions were purified before use by successive passage through columns of alumina and copper under an argon atmosphere. All reagents were purchased from commercial sources, and were used without further purification unless noted otherwise. All reactions were carried out under a positive pressure argon atmosphere and monitored by TLC on Silica Gel G-25 UV_{254} (0.25 mm) unless stated otherwise. TLC spots were detected under UV light and/or by charring with a solution of anisaldehyde in EtOH, acetic acid and H_2SO_4. Column chromatography was performed on Silica Gel 60 (40–60 μm). The ratio between silica gel and crude product ranged from 100:1 to 20:1 (*w*/*w*). Organic solutions were concentrated under vacuum at $<50\,^{\circ}C$. ^1H and ^{13}C NMR spectra were recorded at 700 and 176 MHz, respectively. ^1H and ^{13}C NMR chemical shifts are referenced to CD_3OD ($\delta = 3.35$ and 4.78 for ^1H, 48.9 for ^{13}C). ^1H NMR data are reported as though they are first order and the peak assignments were made on the basis of 2D-NMR (^1H-^1H COSY and HMQC) experiments. ESI-MS spectra were obtained on samples suspended in CH_3OH with added NaCl. Atomic numbering for I-GAZ is shown in Figure 9.

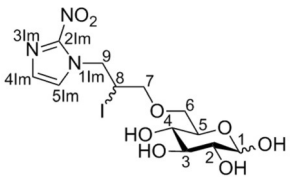

Figure 9. The structure of I-GAZ and atom assignments used for chemical and spectral data.

6-*O*-[9-(2-Nitro-1*H*-imidazolyl)-8-*R*/*S*-iodopropyl]-α/β-D-glucopyranose, I-GAZ: NaI (21.18 mg, 0.14 mmol) was added to a solution of compound **1**[29] (50 mg, 0.07 mmol) in DMF (3 mL), and the reaction mixture was heated at 60 °C for 3 h. The reaction was quenched with H_2O (10 mL) and the product was extracted into EtOAc (10 mL). The organic layer was dried using Na_2SO_4, filtered, and the solvent was removed under reduced pressure. To a solution of the crude product in CH_2Cl_2 (3 mL), 0.1 M methanolic $NaOCH_3$ (3 mL) was added and the solution stirred at 22 °C for 20 min. The reaction mixture was neutralized with Amberlite IR-120 H^+ resin, filtered, and the solvent was removed. The impure product was purified by column chromatography (10:1, *v*/*v*, CH_2Cl_2/CH_3OH) to give I-GAZ (24.2 mg, 74% over two steps) as an amorphous solid: R_f 0.55 (10:1 CH_2Cl_2/CH_3OH); ^1H NMR ($CDOD_3$): $\delta_H = 7.74$ (d, J = 1.0 Hz, H-$4_{\alpha/\beta,\ R/S}$ Im), 7.19 (d, J = 1.1 Hz, H-$5_{\alpha/\beta,\ R/S}$ Im), 5.12 (d, J = 3.7 Hz, H-$1_{\beta,\ R/S}$), 4.49 (d, J = 7.8 Hz, H-$1_{\alpha,\ R/S}$), 4.27 (tt, J = 5.5, 1.9 Hz, H-$9_{\alpha/\beta,\ R/S}$, H-$9'_{\alpha/\beta,\ R/S}$), 4.06 (td, J = 5.5, 2.7 Hz, H-$8_{\alpha/\beta,\ R/S}$, H-$8'_{\alpha/\beta,\ R/S}$), 3.93 (ddd, J = 10.0, 4.8, 2.4 Hz, H-$4_{\beta,\ R/S}$), 3.85 (dd, J = 11.0, 2.0 Hz, H-$6a_{\alpha/\beta,\ R/S}$), 3.78–3.77 (m,H-$5_{\beta,\ R/S}$), 3.73 (dd, J = 11.0, 5.6 Hz, H-$6b_{\alpha/\beta,\ R/S}$), 3.67 (t, J = 9.3 Hz, H-$4_{\alpha,\ R/S}$), 3.46–3.42 (m, H-$5_{\alpha,\ R/S}$)), 3.40–3.34 (m, H-$2_{\beta,\ R/S}$, H-$3_{\alpha/\beta,\ R/S}$, H-$7_{\alpha/\beta,\ R/S}$, H-$7'_{\alpha/\beta,\ R/S}$), 3.16–3.12 ppm (m, H-$2_{\alpha,\ R/S}$); ^{13}C NMR (176 MHz): $\delta_C = 143.50$ and 143.41 (C2 Im), 126.17 and 126.02 (C4 Im), 125.04 and 124.96 (C5 Im), 98.18 ($C1_\alpha$), 93.97 ($C1_\beta$), 78.05 ($C2_\beta$), 76.96 ($C5_\alpha$), 76.19 ($C2_\alpha$), 74.84 ($C4_\alpha$), 73.72 ($C3_\alpha$), 72.07 ($C4_\beta$), 71.83 ($C3_\beta$), 71.65 ($C5_\beta$), 71.12 (C6), 69.56 and 69.49 (C7), 53.16 and 53.10 (C9), 25.08 and 24.90 ppm (C8); HRMS (ESI) calcd for $[M+Na]^+$ $C_{12}H_{18}IN_3O_8Na$: 482.0035, found: 482.003.

Radiolabeling: I-GAZ was radioiodinated by halogen ($^{123/131}$I) exchange under pivalic acid melt conditions (Scheme 1). In a typical reaction, solutions of I-GAZ (100 μg) in EtOH (50 μL) and pivalic acid (1 mg in 50 μL EtOH) were added to a pre-warmed V-vial (heating block; 40 °C) containing Na[^{131}I]I (185 MBq) in methanolic NaOH (100 μL CH_3OH and 2 μL aqueous 0.05 N NaOH). The solvent was evaporated under a gentle stream of argon gas to bring the melt to dryness (~27 min). An additional portion of dry EtOH (100 μL) was added to the vial, and the solvent was again removed under argon. Complete removal of residual traces of water in the reaction mixture was achieved using a high vacuum pump. Anhydrous acetonitrile (CH_3CN; 100 μL) was added to the vial, which was then capped and placed on the pre-heated block heater (100 °C). The reaction was allowed to proceed at this temperature for 2 h, after which the vial was removed from the block heater and cooled to 30 °C. The solvent was removed under a flow of argon, the residue was dissolved in sterile water for injection (SWFI; 200 μL×2), and withdrawn into a syringe. A C_{18} Sep-Pak™ cartridge, preconditioned by flushing with EtOH (2 mL) followed by SWFI (10 mL), and then air-dried by flushing with air (10 mL), was attached to this syringe and the reaction mixture was pushed slowly onto the cartridge; the wash was collected in a vial (iodide vial). The syringe was removed and the cartridge was flushed with SWFI (4 mL) to remove unreacted sodium [^{131}I]iodide, which was also collected in the 'iodide vial' (total 56 MBq). Finally, the cartridge was eluted with 5% EtOH in SWFI (2 mL) to afford the pure radiopharmaceutical, which was collected in a clean pre-evacuated sterile vial. A typical reaction afforded 100 MBq of radiodinated I-GAZ (recovered radiochemical yield; rRCY; 54%) with a radiochemical purity (RCP) > 96% by TLC. TLC radiochromatograms of the 'iodide' and 'product' solutions are shown in Figure 1. [^{123}I]IAZA was prepared by radioiodide exchange with IAZA using a literature technique.[33]

Cytotoxicity: Exponentially-growing murine EMT-6 and human MCF-7 cell cultures (American Type Culture Collection; ATCC; USA) were trypsinized, collected and diluted in the appropriate medium to a cell concentration of 8×10^3 cells per mL. Cells (8×10^2 cells in 100 μL) were seeded into 96-well plates and incubated (24 h; 37 °C) under either 5% CO_2 in air, or under nitrogen. I-GAZ was dissolved at the desired concentrations in growth medium, and the resulting I-GAZ solutions (100 μL) were added to the cell-containing wells. Hypoxic conditions under nitrogen were created by suc-

cessive evacuation/refill cycles with high purity nitrogen. In controls (hypoxic and aerobic), medium (100 μL) replaced the test-compound solution. After a 72 h incubation, 3-(4,5-dimethylthiazol-2-yl)-2,5-diphenyl tetrazolium bromide (MTT, 50 μL of 1 mg mL^{-1} solution) was added to each well, and after a 4 h incubation the supernatant was removed and DMSO (150 μL) was added to each well to dissolve the formazan crystals. The well-plates were shaken for 30 min to ensure complete extraction, then scanned at 540 nm using an ELISA reader. Survival curves (Figure 2) were generated from net (test minus control) optical density data.

Radiosensitization: Human MCF-7 and murine EMT-6 cells (300 000 cells in 3 mL DMEM/F12 medium per T60 glass Petri dish) were incubated (37 °C, 20 h) under 5% CO_2 in air. I-GAZ (stock solution 10 mM in 95% EtOH) was then added to achieve a concentration of 100 μM, and incubation was continued for 24 h. Dishes were assigned to either the control (normoxic) or hypoxic groups. Those in the hypoxic group were de-gassed to hypoxia by six consecutive vacuum/nitrogen (high purity) fill cycles in a vacuum chamber. The Petri dishes (hypoxic and normoxic controls) were then incubated for 30 min on an oscillating shaker at 37 °C (60 cycles/min) and irradiated in a 6 °Co γ-irradiator to 0 (control), 4, 8, 16 and 32 Gy in either N_2 (hypoxic sub-group) or air (normoxic sub-group up to 8 Gy) chambers. The cells were sequentially washed with PBS, trypsinized (500 μL), quenched with fresh medium (4.5 mL), plated in medium at densities ranging from 100 to 15 000 cells per 5 mL medium (normoxic cells; 100 and 5000 cells per 5 mL medium for hypoxic cells), and then incubated (37 °C; 5% CO_2 in air). After 10 to 14 days, cells were stained with methylene blue or crystal violet in EtOH, then clones were counted and surviving fractions calculated. Data are shown in Figure 3.

Hypoxia dependent uptake in vitro: In a separate experiment, [^{131}I]I-GAZ or [^{131}I]IAZA were incubated with EMT-6 cells (10^6 mL) in culture medium under either air (with 5% CO_2) or nitrogen (hypoxic conditions were created by successive evacuation/refill cycles with high purity nitrogen). After 2 h, the cell incubates were treated with trichloroacetic acid (TCA) and the precipitate (bound tracer) was recovered on a fiber filter bed, washed with cold water (2×1 mL) and radioassayed using a γ-counter. Radioactivity uptake data (cpm per well) was transposed for expression as pmol per 10^6 cells.

In vitro cell uptake of [^{123}I]I-GAZ: EMT-6 cells (obtained from Dr. David Murray, Cross Cancer Institute, University of Alberta) were cultured at 37 °C in a humidified atmosphere of 5% (*v*/*v*) CO_2, using DMEM/F12 medium supplemented with 10% fetal bovine serum (FBS), 2 mM L-glutamine and 1% antibiotic/antimycotic (Invitrogen, Burlington, ON, Canada). Cell growth medium was changed every second day and cells were tested against mycoplasma contamination. Exponentially growing cells were sub-cultured into 12-well plates (Corning, Lowell, MA, USA) 24 h before the radiotracer uptake experiment at a density that gave rise to >85% confluence on the experimental day. Before the experiment, the growth medium was removed and the cells were washed once with Krebs–Ringer buffer (120 mM NaCl, 25 mM $NaHCO_3$, 4 mM KCl, 1.2 mM KH_2PO4, 2.5 mM $MgSO_4$, 70 μM $CaCl_2$, pH 7.4). The cells were subsequently incubated in Krebs–Ringer buffer for 1 h before radiotracer incubation was started. The radiotracer [^{123}I]I-GAZ was diluted in either Krebs–Ringer buffer with or without addition of 5 mM glucose to ~500 kBq per mL buffer solution. Cells were incubated with [^{123}I]I-GAZ containing buffer solution at 37 °C for 1 min up to 90 min. Radiotracer uptake was stopped at dedicated time points by washing the cells with ice-cold Krebs–Ringer buffer twice. Cells were lysed with 5% (TCA) at 37 °C for 5 min and transferred into scintillation vials. The cell lysate was counted in a γ-counter (Wallac 1480 Wizard-3, PerkinElmer, Canada). Protein levels were quantified using the BCA protein assay kit (Pierce, Rockford, IL, USA) according to the manufacturer's recommendations; bovine serum albumin was used as the protein standard. Cell uptake levels were normalized to percent of the total added amount of radioactivity corresponding to exposure dose (%ED) per mg protein (Figure 4).

Biodistribution of [^{131}I]I-GAZ in subcutaneous EMT-6 tumors bearing Balb/c mice: The animal experiments were carried out in accordance with guidelines of the Canadian Council on Animal Care (CCAC), and were approved by the local animal care committee of the Cross Cancer Institute. Murine EMT-6 cells (5×10^6 cells in 100 μL PBS) were injected into the upper left flank of female Balb/c mice (20–24 g, Charles River, Canada). The biodistribution experiment was performed after allowing 8 to 11 days for the tumors to grow. The EMT-6 tumors analyzed in this study reached final sizes of 171.5 ± 9.8 mg (n = 15). After intravenous (i.v.) injection of [^{131}I]I-GAZ (170–190 kBq in 100 μL saline) into the tail vein of isoflurane anesthetized mice, the animals were allowed to regain consciousness until sacrifice. Animals were euthanized in a CO_2 chamber at 5, 30, 60 min and at 4 and 24 h post-injection, and then rapidly dissected. Organs of interest (blood, heart, lung, liver, kidneys, gall bladder, spleen, stomach, duodenum, small and large intestines, pancreas, right femur, muscle, ovaries, brain, fat, thyroid and tumors) were collected and weighed. Radioactivity in all tissue samples was measured in a γ-counter and results were analyzed as percentage of injected dose per gram (%ID/g) of tissue (Table 1).

Acknowledgements

The authors thank Dr. Melinda Wuest for her help with the biological studies and related data analyses. E.L. was supported in part by a Postgraduate Overseas Research Experience Scholarship and by Dr. Uwe Ackerman (University of Melbourne. B.Z. held an Alberta Cancer Foundation Summer Studentship (ACF 25966). We thank Kayleigh Wiebe for technical assistance. This project was funded in part by grants from the Canadian Institutes for Health Research (POP Phase I, G118980046; L.I.W.), the Alberta Cancer Foundation (grant 25141, P.K.), and from Alberta Innovates—Health Solutions (CRIO Program grant 101201164, P.K.).

Keywords: antitumor agents · azomycin · glycoconjugates · iodination · tumor hypoxia

[1] N. Sadri, P. J. Zhang, *Cancers* **2013**, *5*, 320–333.
[2] B. Nath, G. Szabo, *Hepatology* **2012**, *55*, 622–633.
[3] G. L. Semenza, *Annu. Rev. Phytopathol.* **2014**, *9*, 47–71.
[4] C. M. Girgis, K. Cheng, C. H. Scott, J. E. Gunton, *Trends Endocrinol. Metab.* **2012**, *23*, 372–380.
[5] X. Zhao, Y. Yue, W. Cheng, J. Li, Y. Hu, L. Qin, P. Zhang, *Curr. Drug Targets* **2013**, *14*, 700–707.
[6] G. E. Adams, D. L. Dewey, *Biochem. Biophys. Res. Commun.* **1963**, *12*, 473–477.
[7] G. E. Adams, I. R. Flockhart, C. E. Smithen, I. J. Stratford, P. Wardman, M. E. Watts, *Radiat. Res.* **1976**, *67*, 9–20.
[8] K. Liu, H. L. Zhu, *Anti-Cancer Agents Med. Chem.* **2011**, *11*, 687–691.
[9] L. I. Wiebe in *Imaging of Hypoxia: Tracer Developments* (Ed.: H.-J. Machulla), Kluwer Academic, Dordrecht, **1999**, pp. 155–176.
[10] L. I. Wiebe, A. J. B. McEwan, *Braz. Arch. Biol. Technol.* **2002**, *45*, 69–81.
[11] K. A. Krohn, J. M. Link, R. P. Mason, *J. Nucl. Med.* **2008**, *49*, 129S–148S.

[12] L. Hoigebazar, J. M. Jeong, *Recent Results Cancer Res.* **2013**, *194*, 285 – 299.
[13] P. Kumar, V. Bacchu, L. I. Wiebe, *Semin. Nucl. Med.* **2015**, *45*, 122 – 135.
[14] C. L. Ricardo, P. Kumar, L. I. Wiebe, *J. Diagn. Imaging Ther.* **2015**, *2*, 103 – 158.
[15] P. Wardman, *J. Clin. Oncol.* **2007**, *19*, 397 – 417.
[16] S. T. Lee, A. M. Scott, *Semin. Nucl. Med.* **2007**, *37*, 451 – 461.
[17] G. B. Halmos, L. Bruine de Bruin, J. A. Langendijk, B. F. van der Laan, J. Pruim, R. J. Steenbakkers, *Clin. Nucl. Med.* **2014**, *39*, 44 – 48.
[18] E. J. Postema, A. J. B. McEwan, T. A. Riauka, P. Kumar, D. A. Richmond, D. N. Abrams, L. I. Wiebe, *Eur. J. Nucl. Med. Mol. Imaging* **2009**, *36*, 1565 – 1573.
[19] R. C. Urtasun, M. B. Parliament, A. J. McEwan, J. R. Mercer, R. H. Mannan, L. I. Wiebe, C. Morin, J. D. Chapman, *Br. J. Cancer* **1996**, *74*, S209 – S212.
[20] E. O. Aboagye, A. D. Lewis, M. A. Graham, M. Tracy, A. B. Kelson, K. J. Ryan, P. Workman, *Anti-Cancer Drug Des.* **1996**, *11*, 231 – 242.
[21] D. M. Brown, N. Y. Yu, J. M. Brown, W. W. Lee, *Int. J. Radiat. Oncol. Biol. Phys.* **1982**, *8*, 435 – 438.
[22] L. I. Wiebe, D. Stypinski, *Q. J. Nucl. Med.* **1996**, *40*, 270 – 284.
[23] S. Emami, P. Kumar, J. Yang, Z. Kresolic, R. Paproski, C. Cass, A. J. McEwan, L. I. Wiebe, *J. Pharm. Pharm. Sci.* **2007**, *10*, 237 – 245.
[24] G. E. Adams, I. Ahmed, E. D. Clarke, P. O'Neill, J. Parrick, I. J. Stratford, R. G. Wallace, P. Wardman, M. E. Watts, *Int. J. Radiat. Biol. Relat. Stud. Phys. Chem. Med.* **1980**, *38*, 613 – 626.
[25] S. Dische, *Radiother. Oncol.* **1985**, *3*, 97 – 115.
[26] A. Habr-Gama, R. O. Perez, G. P. São Julião, I. Proscurshim, J. Gama-Rodrigues, *Anti-Cancer Drugs* **2011**, *22*, 308 – 310.
[27] N. Malik, L. Xian, D. Löffler, B. Shen, C. Solbach, G. Reischl, W. Voelter, H.-J. Machulla, *J. Radioanal. Nucl. Chem.* **2012**, *292*, 1025 – 1033.
[28] M. Patt, D. Sorger, M. Scheunemann, G. Stocklin, *Appl. Radiat. Isot.* **2002**, *57*, 705 – 712.
[29] P. Kumar, G. Shustov, H. Liang, V. Khlebnikov, W. Zheng, X.-H. Yang, C. Cheeseman, L. I. Wiebe, *J. Med. Chem.* **2012**, *55*, 6033 – 6046.
[30] M. Wuest, P. Kumar, M. Wang, J. Yang, H.-S. Jans, L. I. Wiebe, *Cancer Biother. Radiopharm.* **2012**, *27*, 473 – 480.
[31] L. F. Barros, C. X. Bittner, A. Loaiza, I. Ruminot, V. Larenas, H. Moldenhauer, M. Oyarzun, M. Alvarez, *J. Neurochem.* **2009**, *109*, 94 – 99.
[32] N. C. Denko, *Nat. Rev. Cancer* **2008**, *8*, 705 – 713.
[33] R. H. Mannan, V. V. Somayaji, J. Lee, J. R. Mercer, J. D. Chapman, L. I. Wiebe, *J. Nucl. Med.* **1991**, *32*, 1764 – 1770.
[34] J. V. Watson, P. Workman, S. H. Chambers, *Br. J. Cancer* **1978**, *37*, 397 – 402.
[35] J. P. Weichert, M. E. Van Dort, M. P. Groziak, R. E. Counsell, *Int. J. Radiat. Appl. Instrum. Part A. Appl. Radiat. Isot.* **1986**, *37*, 907 – 913.
[36] G. E. Adams, I. J. Stratford, *Biochem. Pharmacol.* **1986**, *35*, 71 – 76.
[37] G. F. Whitmore, A. J. Varghese, *Biochem. Pharmacol.* **1986**, *35*, 97 – 103.
[38] T. Kagiya, S. Nishimoto, Y. Shibamoto, J. Wang, L. Zhou, Y. L. He, K. Sasai, M. Takahashi, M. Abe, *Int. J. Radiat. Oncol. Biol. Phys.* **1989**, *16*, 1033 – 1037.
[39] S. M. Eschmann, F. Paulsen, M. Reimold, H. Dittmann, S. Welz, G. Reischl, H.-J. Machulla, R. Bares, *J. Nucl. Med.* **2005**, *46*, 253 – 260.
[40] M. Piert, H.-J. Machulla, M. Picchio, G. Reischl, S. Ziegler, P. Kumar, H.-J. Wester, R. Beck, A. J. McEwan, L. I. Wiebe, M. Schweiger, *J. Nucl. Med.* **2005**, *46*, 106 – 113.

Received: April 20, 2016
Revised: June 6, 2016
Published online on July 5, 2016

